

Supplementary Information: Revealing nanoscale slip within Taylor-Aris dispersion[†]

Mehul Bapat,^a Gerald J. Wang^{*a}

1 Shear-augmented diffusivity with slip boundary conditions

In this section, we derive the expression for the streamwise-to-spanwise diffusivity ratio. Using the same plane-Couette setup shown in figure 1, the Navier-Stokes equations for the steady and fully developed flow in the x -direction is:

$$\frac{\partial^2 u}{\partial z^2} = 0, \text{ with boundary conditions} \quad (1a)$$

$$u(z=0) = -(u_w - u_s) \text{ and} \quad (1b)$$

$$u(z=H) = (u_w - u_s), \text{ with solution} \quad (1c)$$

$$u(z) = (u_w - u_s) \left(\frac{2z}{H} - 1 \right) \quad (1d)$$

We consider the concentration c of a set of reference tracers within the fluid. Assuming c varies only in the x - and z -directions, advection-diffusion gives¹:

$$\frac{\partial c}{\partial t} + u \frac{\partial c}{\partial x} = D_{\text{eq}} \left(\frac{\partial^2 c}{\partial x^2} + \frac{\partial^2 c}{\partial z^2} \right) \quad (2a)$$

Assuming impermeability of the walls,

$$\left. \frac{\partial c}{\partial z} \right|_{z=0} = \left. \frac{\partial c}{\partial z} \right|_{z=H} = 0. \quad (2b)$$

We can decompose the concentration $c(x, z, t)$ as a sum of its cross-sectional average $\bar{c}(x, t)$ and its z -varying component $c'(x, z, t)$:

$$c(x, z, t) = \bar{c}(x, t) + c'(x, z, t), \text{ where} \quad (3a)$$

$$\bar{c}(x, t) = \frac{1}{H} \int_0^H c(x, z, t) dz, \text{ thereby requiring} \quad (3b)$$

$$\frac{1}{H} \int_0^H c'(x, z, t) dz = 0. \quad (3c)$$

The cross-sectional average of (2a) with (2b), (3a), (3b), and (3c) yields:

$$\frac{\partial \bar{c}}{\partial t} + \frac{1}{H} \int_0^H u \frac{\partial c'}{\partial x} dz = D_{\text{eq}} \left(\frac{\partial^2 \bar{c}}{\partial x^2} \right). \quad (4)$$

The difference between (4) and (2a) implies:

$$\frac{\partial c'}{\partial t} + u \frac{\partial \bar{c}}{\partial x} + u \frac{\partial c'}{\partial x} - \frac{1}{H} \int_0^H u \frac{\partial c'}{\partial x} dz = D_{\text{eq}} \left(\frac{\partial^2 c'}{\partial x^2} + \frac{\partial^2 c'}{\partial z^2} \right). \quad (5a)$$

To further simplify (5a), we make two observations: (i) after a time that is $\mathcal{O}(H^2/D_{\text{eq}})$, diffusion will smooth out variations in the z -direction, such that $\bar{c} \gg c'$ and $(\partial c'/\partial t)$ vanishes and (ii) $(\partial^2 c'/\partial x^2) \ll (\partial^2 c'/\partial z^2)$ and $(\partial c'/\partial x) \approx 0$. As a consequence:

$$u \frac{\partial \bar{c}}{\partial x} = D_{\text{eq}} \left(\frac{\partial^2 c'}{\partial z^2} \right). \quad (5b)$$

Combining (5b) with the velocity profile (1d), boundary conditions (2b), and cross-sectional average (3c), we can isolate the z -varying part of the concentration:

$$c'(x, z, t) = \frac{(u_w - u_s)}{12HD_{\text{eq}}} \frac{\partial \bar{c}}{\partial x} (4z^3 - 6Hz^2 + H^3) \quad (5c)$$

With this, (4) reduces to:

$$\frac{\partial \bar{c}}{\partial t} = \left[D_{\text{eq}} + \frac{(u_w - u_s)^2 H^2}{30D_{\text{eq}}} \right] \frac{\partial^2 \bar{c}}{\partial x^2}, \quad (6a)$$

where the bracketed pre-factor can be identified as the shear-augmented (effective) diffusivity D_{eff} , thereby implying:

$$\frac{D_{\text{eff}}}{D_{\text{eq}}} = 1 + \frac{(u_w - u_s)^2 H^2}{30D_{\text{eq}}^2}. \quad (7)$$

2 Dependence of equilibrium diffusivity on viscosity and polymer chain length

As shown in fig 1a, MD results for the spanwise diffusivity D_{eq} as a function of chain length N_m are in general agreement with the $-3/2$ power scaling observed for polymers near an interface². In figure 1b, we show the viscosity μ of different fluids as a function of the chain length, which indicates that viscosity scales linearly with chain length (as expected in the pre-entanglement regime). As a consequence of these observations, we conclude $D_{\text{eq}} \sim \mu^{-3/2}$ for our systems of confined polymers.

3 Long-chain polymers and Taylor-Aris dispersion

We performed additional simulations for $N_m \in \{20, 25, 30\}$ for a gap height of $H = 15.9$. As shown in figure 2a, the slip velocity inferred from Taylor-Aris dispersion is in good agreement with that measured from the velocity profiles for longer chain lengths. There is another trend worth noting: As the polymer chain length increases (while holding the interaction between the wall and each monomer fixed), the slip velocity also increases, eventually saturating at the maximum possible value of the slip velocity, i.e., the wall velocity u_w (put another way, the mismatch between the wall velocity and the interfacial fluid velocity is bounded from above by the wall velocity itself). In figure 2b, we observe that when $N_m \gtrsim 10$, the slip velocity is near saturation to the wall velocity.

4 Effect of thermostats on Taylor-Aris dispersion

Previous work has shown that holding the walls as rigid and applying the thermostat only to the fluid tends to reduce the slip velocity measured in MD³. In figure 3, we show slip velocity measured from the velocity profile and inferred from Taylor-Aris dispersion ($N_m = 3$, $u_w = 0.52$, and thermodynamic and geomet-

^a Department of Civil and Environmental Engineering, Carnegie Mellon University, Pittsburgh, PA 15213, USA.; E-mail: gjwang@cmu.edu

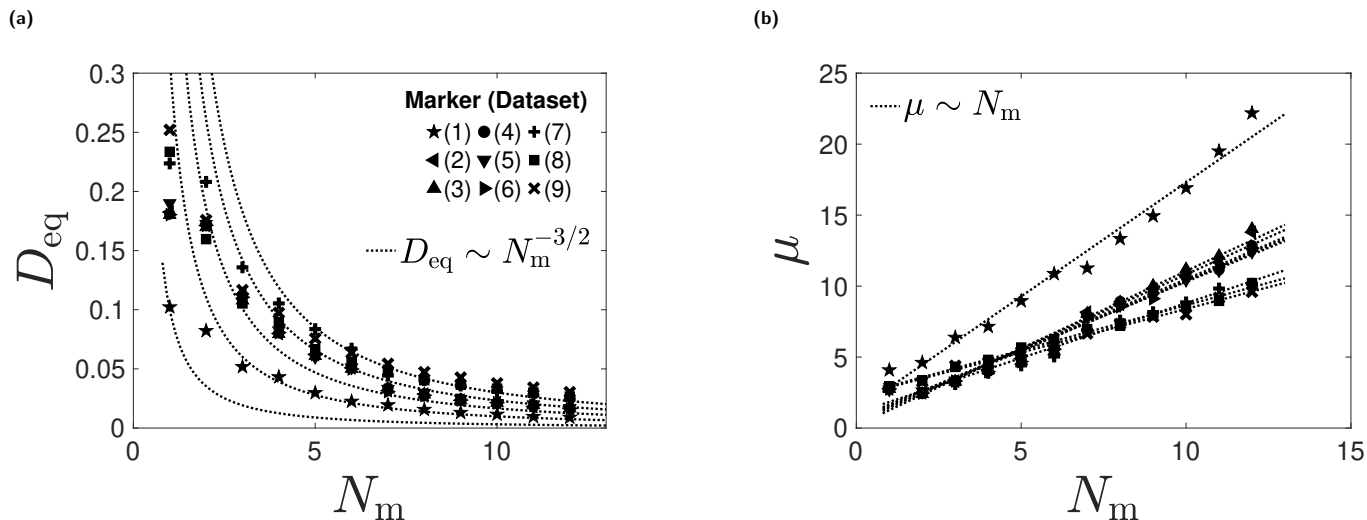


Fig. 1 (a) For the fluids simulated in our study, equilibrium diffusivity, D_{eq} as a function of number of monomers in each chain N_m , along with the contours of the scaling observed in previous literature² overlaid. (b) Viscosity as a function of number of monomers in each chain. Dashed lines representing contours of the scaling in the legend are overlaid.

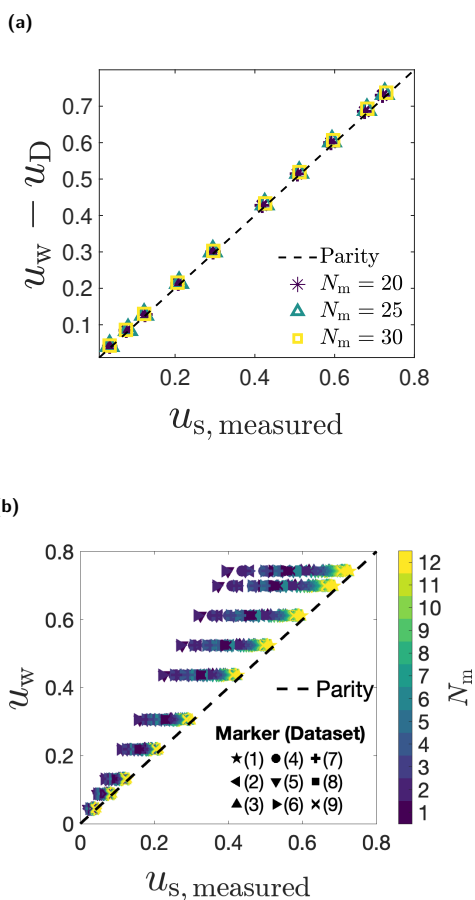


Fig. 2 (a) Slip velocity measured using MD simulations vs. that inferred from Taylor-Aris dispersion for polymer chain lengths of 20, 25 and 30, for the thermodynamic and geometric conditions from dataset 4 in the manuscript. (b) A comparison of magnitude of wall velocity against the measured slip velocity for LJ fluids presented in the manuscript.

ric conditions from dataset 4) for three choices of thermostat use and for a range of thermostat damping timescales (following the damping timescale conventions used in LAMMPS⁴ for each of these thermostats). In particular, we simulate: (1) rigid walls and a Nosé-Hoover thermostat^{5,6} applied only to the fluid (Fluid-NH); (2) rigid walls and a Langevin thermostat⁷ applied only to the fluid (Fluid-LT); and (3) flexible walls with a Nosé-Hoover thermostat only applied to the walls, following the approach of Bernardi *et al.*³ (Walls-NH). We find that even though each of these choices with regard to thermostat usage has the potential to affect the slip velocity, it also commensurately modifies the diffusion coefficients such that the Taylor-Aris dispersion approach still yields a slip velocity in agreement with the traditional measurement approach (deviations from parity on the order of 5% or less).

Notes and references

- 1 R. Bird, W. Stewart and E. Lightfoot, 2002.
- 2 S. A. Sukhishvili, Y. Chen, J. D. Müller, E. Gratton, K. S. Schweizer and S. Granick, *Macromolecules*, 2002, **35**, 1776–1784.
- 3 S. Bernardi, B. D. Todd and D. J. Searles, *The Journal of Chemical Physics*, 2010, **132**, 244706.
- 4 A. P. Thompson, H. M. Aktulga, R. Berger, D. S. Bolintineanu, W. M. Brown, P. S. Crozier, P. J. in 't Veld, A. Kohlmeyer, S. G. Moore, T. D. Nguyen, R. Shan, M. J. Stevens, J. Tranchida, C. Trott and S. J. Plimpton, *Comp. Phys. Comm.*, 2022, **271**, 108171.
- 5 S. Nosé, *The Journal of chemical physics*, 1984, **81**, 511–519.
- 6 W. G. Hoover, *Physical review A*, 1985, **31**, 1695.
- 7 T. Schneider and E. Stoll, *Phys. Rev. B*, 1978, **17**, 1302–1322.

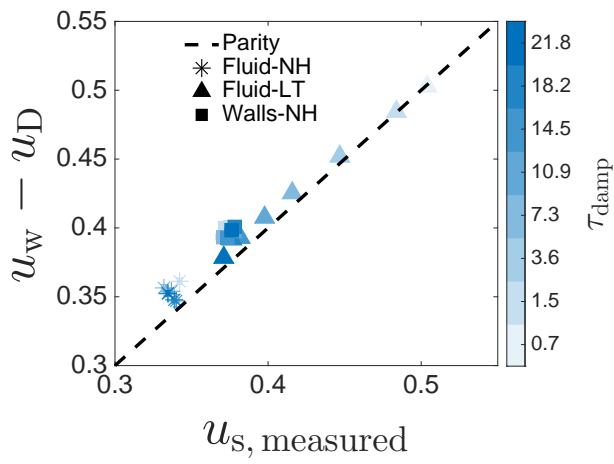


Fig. 3 For a fluid with polymer chain length $N_m = 3$ at a wall velocity $u_w = 0.52$ from dataset 4, slip velocity measured using Taylor-Aris dispersion (vertical axis) and using the velocity profile (horizontal axis) is shown for three distinct thermostat approaches (symbols) and a range of values for the thermostat damping timescale τ_{damp} (colorbar): (*) Fluid-NH indicates a Nosé-Hoover thermostat applied to the fluid only and walls held rigid; (▲) Fluid-LT indicates a Langevin thermostat applied to the fluid only and walls held rigid; (■) Walls-NH indicates flexible walls and a Nosé-Hoover thermostat applied only to the walls. Parity is shown as a dashed line.